

Simplicity on the other side of ecological complexity

Eric L. Berlow^{1,2,3}, Jennifer A. Dunne^{4,3}, Neo D. Martinez³, Philip B. Stark⁵, Richard J. Williams^{6,3}, and Ulrich Brose^{2,3}

¹ *University of California, Merced, Sierra Nevada Research Institute, Wawona Station, Yosemite National Park, CA 95389 USA*

² *Darmstadt University of Technology, Department of Biology, Schnittspahnstr. 10, 64287 Darmstadt, Germany*

³ *Pacific Ecoinformatics and Computational Ecology Lab, Rocky Mountain Biological Lab, POB 519, Gothic, CO 81224 USA*

⁴ *Santa Fe Institute, 1399 Hyde Park Road, Santa Fe, NM 87501 USA*

⁵ *University of California Berkeley, Department of Statistics, Berkeley, CA 94720-3860 USA*

⁶ *Microsoft Research Ltd, 7 J. J. Thomson Avenue, Cambridge CB30FB UK*

Darwin's classic image of a 'tangled bank' of interdependencies among species has long suggested the difficulty of predicting how the loss of one species alters the abundance of others¹. We show that for dynamical models of realistically structured ecological networks in which pair-wise consumer-resource interactions scale according to allometric $3/4$ power rules suggested by metabolic theory^{2,3}, the effect of losing one species on another typically can be predicted surprisingly well by simple functions of variables that can be observed in nature. By systematically removing individual species from 600 10-30 species networks, we analyzed how the sign and magnitude of 254,032 possible pair-wise species interactions depended on 90 stochastically varied species, link, and network attributes. Population-level and

***per capita* effects of removing one species on the biomass change of another do not vary according to the simple allometric rules that govern pair-wise trophic interactions. Instead, the exponent of the relationship between the removed species body mass and *per capita* interaction strength is almost twice as large due to network effects. The maximum interaction strength decreases exponentially as the degree of separation between the target and removed species increases. The sign of strong interactions is predicted well by a weighted sum of the signs of the shortest and next-shortest paths between the removed and target species. The magnitude of positive and negative interactions is predicted well by the two species' biomasses. Perhaps most surprisingly, it is easier to predict interactions for larger webs: greater web complexity may simplify predicting ecological dynamics⁴ as evidenced by the greater ease of predicting interaction strengths in larger webs. Applied to field data, our model successfully predicts interactions dominated by trophic effects and illuminates the sign and magnitude of important non-trophic interactions.**

"I would not give a fig for simplicity on this side of complexity, but I'd give my life for the simplicity on the other side of complexity" -- Oliver Wendell Holmes Jr.

One of the greatest challenges of environmental biology is to predict the effect of human activity on the complex webs of interactions among species. There has been theoretical progress understanding how the extinction of one species can cause some other species to go secondarily extinct⁵⁻⁸, but knowing how extinctions affect the abundances of *all* species in a community is critical for predicting community responses to external perturbations^{9,10}. Many species interactions involve the fundamental need to acquire energy, and well-documented allometric scaling rules describe relationships between body size, metabolism^{11,12}, and food consumption^{2,13}. What do these scaling rules imply about the effect of removing one species on others in a realistically

structured food web? Non-trophic interactions among species, such as habitat modification, interference competition, and behavioural modifications^{14,15} also affect species abundances, but the fundamental physiological need for food can provide a null model¹⁶ of species interactions against which the importance of other ecological processes can be assessed.

Here, we report numerical experiments that explore how extinctions affect the abundances of all other species in models of complex food webs. We simulated population dynamics and species removals in 600 food web models with 10-30 species and where all pair-wise consumer-resource trophic interactions are governed by simple allometric scaling rules^{5,17,18}. We explore two general questions: 1) How are *per capita* pair-wise rules modified by network dynamics? 2) Is there a simple predictor of the dynamic effect of removing a species on the other species in a network governed by simple allometric scaling rules?

The models are based on five simplifying assumptions: 1) autotrophs or “basal species” compete for fixed inputs of two primary limiting nutrients, 2) the rate of metabolism and maximum *per capita* consumption (hereafter, “maximum consumption”) of all consumers scale with their body mass to the $\frac{3}{4}$ power^{2,3}, 3) consumer-resource body-mass ratios are log-normally distributed with mean 10 and standard deviation 100^{ref.19}, 4) networks are structured according to the “niche model”²⁰, and 5) generalist consumers feed on different resources in proportion to the resources' relative biomasses (i.e., there is no complex foraging behaviour). This *Allometric-Trophic-Network (ATN)* model makes it possible to more generally explore how any scaling relationships for bioenergetics and feeding interactions manifest in a network context.

We generated 600 food web models, ranging from 10 to 30 species, with realistic stochastic variation in network structure and species attributes that drive population dynamics. For each web, we simulated the effect of removing each species in turn

(hereafter R , or “removed species”) on the biomass of every other species in the web (hereafter T , or “target species”). Simulated species’ biomass and population density fluctuate indefinitely but their averages over moderate time windows stabilize after an initial transient phase (see Supplement). Removal effects are measured using these averages as either *population-level* interaction strengths ($I = T_{biomass}$ with R minus $T_{biomass}$ without R) or *per capita* interaction strengths (*per capita* $I = \text{population } I$ divided by $R_{density}$).

We focus on the strength of dynamic coupling between R and T , rather than on the number of secondary extinctions^{6-8,21} or the change in T ’s variance caused by removing R ^{ref.22} (see Supplementary Material). We simulated all possible 254,032 interactions between R and T across all degrees of separation in the 600 networks while recording 90 network and species attributes for each interaction (see Full Methods). Of the interactions in these species-removal simulations, 45% were positive and 55% were negative. Consistent with empirical findings, there was a negative power law between mean species density and body mass¹¹ (Supplementary Fig. S4); the distributions of both positive and negative I and *per capita* I were all approximately log-normal (Supplementary Fig. S4)^{9,23,24}; and the maximum I decreased with increasing degrees of separation between R and T quantified as the shortest path length between them (Fig. 1a).

We explored how well a simple model based on a small subset of attributes could predict the effect of removing one species on others. We used a Classification and Regression Tree (CART) algorithm to model the magnitude and sign of I in a random sample of 300 of the food networks (training data) as a function of the 90 explanatory variables (see Full Methods). Since the distribution of both positive and negative I is roughly lognormal, this CART for raw I is dominated by the strongest interactions, a subject of long-standing scientific interest (see Full Methods). CART explains 86% of

the variation in I in the training data and 89% in the other 300 food networks (test data) using 7 of the 90 variables. Combinations of these variables classify groups of interactions whose mean strength was within the top 5% of interaction strengths (Fig. 1a-c coloured symbols). The strongest negative interactions among these groups are one-degree effects of R on basal T that have R as their only consumers (Fig. 1a-c, red symbols). More generally, strong positive and negative interactions are associated with: high biomass ($> 75^{\text{th}}$ percentile) of R and T (with R present), low degrees of separation, and “simply connected” species (in contrast to diffusely connected species with >1 path between them) (Fig. 1). The sign of interactions is predicted best by a weighted sum of the signs of the shortest and next-shortest paths from R to T (see Full Methods). Species with one- and two-degree interactions are often connected by longer paths as well, but our simulations support the proposition that longer paths have less influence than shorter paths^{14,25}. CART used different variables to predict the magnitude and sign of I . Modelling $\log|I|$ instead of I reveals a simpler pattern: $\log|I|$ varies approximately linearly with $\log(R_{\text{biomass}})$ and $\log(T_{\text{biomass}})$ (Fig. 1d). CART explains 66% of the variance in $\log|I|$ in the training data and 63% in the test data. Thus, the strong interactions explained by the CART model for raw I (Fig. 1 c, coloured symbols) are part of a broader pattern among all interactions. A linear model for $\log|I|$ as a function of $\log(T_{\text{biomass}})$ and $\log(R_{\text{biomass}})$ also accounts for 65% of the variance in $\log|I|$ in the training data and 63% in the test data (Fig. 1d). Including degrees of separation as an explanatory variable accounts for an additional 1% of the variance in $\log|I|$. The other four variables CART used to model raw I (Fig. 1a-c; the weighted sum of signs, simple vs. diffuse interactions, T trophic level, and the number of T 's direct consumers) explain less than 0.5% more of the variance of $\log|I|$.

These results suggest that strong interactions are primarily associated with high R and T biomass (with R present) and secondarily with low degrees of separation. To test whether the strong correlation between $\log|I|$ and $\log(T_{\text{biomass}})$ is an artifact of the

definition of I ($T_{biomass}$ with R minus $T_{biomass}$ without R), we shuffled $T_{biomass}$ randomly, computed I from the reshuffled data, and computed the correlation of those artificial values of $\log|I|$ and $\log(T_{biomass})$. The largest absolute Pearson correlation for 10,000 random permutations was 0.44, considerably smaller than the Pearson correlation of the original data, 0.77. One might expect that, for negative effects, rare T should increase the most following species loss, but our simulations show the opposite.

We expect from metabolic theory that *per capita* I be universally constrained by the power-law scaling of metabolism and consumption with body mass²⁴. In our ATN simulations, log maximum *per capita* consumption was modelled to vary linearly with log consumer body mass. The slope of the relationship is $\frac{3}{4}$, and the intercept decreases with generality as a consumer divides its consumption among more resource species (Fig. 2a). Stochastic variation in species' generality yields an overall slope of 0.74 (Fig. 2a). Other theoretical studies have used a measure of “interaction strength” that is comparable to the maximum *per capita* consumption described here^{13,26,27}. To explore how this $\frac{3}{4}$ scaling of individual consumption manifests as *per capita* effects of removing R , we first regressed $\log_{10}|per\ capita\ I|$ on $\log_{10}(R_{body_mass})$. Simple, one degree consumer-resource interactions (i.e., effects of specialist consumers on resources with only one consumer) preserve this allometric scaling relationship (slope = 0.74, $R^2 = 0.32$). However, for diffuse, one degree consumer-resource interactions, the slope increases to 1.30 ($R^2 = 0.16$). When all possible pair-wise interactions are included, the regression predicts 46% of the variance in $\log|per\ capita\ I|$ (Fig. 2b), but the exponent of this relationship, 1.38, is almost double the expected exponent of 0.74 (Fig. 2a). Of the 89 other variables we tracked, $R_{biomass}$ and $T_{biomass}$ with R present explain 61% of the remaining variance of $\log|per\ capita\ I|$. Linear regression using $\log(R_{body_mass})$, $\log(R_{biomass})$, and $\log(T_{biomass})$ accounts for 88% of the variance of $\log|per\ capita\ I|$ for both the training and test data (Fig. 2c). Including the $R_{biomass} \times T_{biomass}$ interaction accounts for less than 0.2% more. Thus, $\frac{3}{4}$ allometric scaling of *per capita* I with

R_{body_mass} is only preserved for the simplest possible consumer-resource interactions. In a network context strong *per capita* interactions tend to be between large, low biomass R and high biomass T .

In our simulations, $|I|$ and *per capita* $|I|$ are predicted well by linear models that include the time-averaged biomasses of R and of T as explanatory variables. Predictions using the biomass at a single time would be less accurate if the biomass fluctuates rapidly. Prior analyses of “keystone” species removal in complex networks⁵ focused on one type of positive interaction where the removal of a consumer, R , causes a strong increase in a competitively dominant basal T that, in turn, causes other basal T species to go secondarily extinct. The group of red symbols in Figure 1a-c represent the small subset of cases where a dominant basal T increases greatly when its only consumer is removed. In cases of secondary extinction of $T^{ref.5}$, I has been shown to depend strongly on local network structure with R present. In the more general case explored here where $T_{biomass}$ absent R is non-zero, these local network properties do not help much to predict I : attributes of T and R suffice.

In summary, our ATN simulations elucidate how very general metabolic constraints on trophic relationships play out when consumer-resource interactions are embedded in realistically structured networks. In a complex network, the response of one species to the removal of another does not scale the same way that direct *per capita* feeding interactions do. However, new simple patterns emerge. Our results were consistent across wide variation in network structure, consumer-resource body mass ratios, consumer functional responses, and other species traits used to model species’ population dynamics. These simulations also suggest that in trophic networks, static measures of interaction strengths based on simple species attributes (e.g., body mass and biomass)^{9,13} may be highly correlated with dynamic measures based on removing species. More complex networks had simpler behaviour: the proportion of variation in

both I and *per capita I* explained by the set of simple R and T attributes increased approximately linearly with species richness (Fig. 3). ATN simulations characterize the behaviour of networks connected by metabolically constrained trophic interactions. Deviations from that “ideal” behaviour in natural communities should elucidate the importance of non-trophic interactions and non-metabolic processes on species abundances. The selected variables that best predict interaction sign and magnitude in the ATN simulations are easily measured in “intact” communities, which facilitates predicting the consequences of species loss for other species’ biomasses in field settings.

We illustrate this idea using a field experiment that disentangled trophic and non-trophic interactions in a rocky intertidal community^{22,28}. The experiment manipulated three species in a network of about 30 species that varied naturally over space and time (see Full Methods). This study experimentally separated primarily trophic effects of R on T from well-known strong non-trophic effects mediated by a third species (Fig. 4 a vs. b). In this system, R is a predatory whelk and T is its sessile mussel prey. Both positive and negative non-trophic effects of whelks on mussels are mediated by barnacles. Barnacles facilitate mussel recruitment: they are a preferred settlement substrate^{22,28}. Whelks consume barnacles, but can also help them survive physical disturbances by thinning very dense colonies²².

When barnacles are excluded, the central tendency of *per capita I* of whelks on mussels (Fig. 4 a solid lines) is consistent with the linear model from our ATN simulations (Fig. 4 a dotted lines). Both regressions explain 48% of the variation in \log *per capita I*. However, when barnacles introduce non-trophic effects, our metabolic-trophic model under-predicts *per capita I* at low mussel biomass and over-predicts *per capita I* at very high mussel biomass (Fig. 4b). The difference between observed I and that predicted by our metabolic-trophic model is explained well by natural variation in barnacle cover

(Fig. 4c). The observed negative effects of whelks on mussels were stronger than the model predicts when barnacles cover was low ($< \sim 50\%$), and weaker than predicted when barnacle cover was high ($> \sim 75\%$) (Fig. 4c). At low natural barnacle cover, the non-trophic effect of whelks on mussels is negative because whelks reduce the abundance of barnacles, impeding mussel recruitment. At very high barnacle cover, however, the non-trophic effect of whelks on mussels is positive because whelks stabilize barnacle abundance, which increases mussel recruitment. In sum, the ATN model accurately predicts the effect of whelks on mussels, absent non-trophic facilitation by barnacles. Deviations from the ATN model predictions reveal both the magnitude and sign of the important non-trophic effect. Results for population-level I are similar (data not shown).

Our ATN simulations show how network effects transform a simple allometric rule for pair-wise feeding interactions. The approach could be extended to incorporate additional ecological factors^{7,29} to describe an energetic baseline of species interactions in ecosystems that vary in the importance of environmental stochasticity and spatial and sub-population scale processes. The predictability of simulated interactions suggests that: 1) field studies of interactions that focus on a simple subset of a natural community provide insights that are robust to variation in peripheral network structure; 2) species' interactions known to be driven by energetics may be predicted well by simple species and network attributes; and 3) the characteristic variability, or "context-dependency," of species' interaction strengths in empirical studies²³ may not be due to intractable network influences¹. Instead, this variability may point to other biotic mechanisms including non-trophic interactions or abiotic factors regulating species abundances^{14,15}. Metabolic requirements are critical to all ecological networks, and the predictability of interactions mediated by these requirements makes it possible to assess the relative importance of other ecological processes by examining deviations from ATN

predictions¹⁶. Our results suggest that the complexity of natural food webs is tractable and may simplify, rather than complicate, predicting the consequences of species loss.

Methods Summary

We employ four steps to simulate Allometric-Trophic-Networks (ATN): (1) The niche model²⁰ generates network structures with random, uniformly distributed species richness (10 to 30) and connectance (0.1-0.2). (2) Species' body masses are generated, starting with a basal species level of unity. Successively higher levels are generated using average consumer-resource body-mass ratios sampled from a log-normal distribution (mean = 10, SD = 100)^{17,19}. (3) A dynamic consumer-resource model³ is parameterized by random initial biomasses and $\frac{3}{4}$ power-law relationships between the rates of metabolism, maximum consumption and production and body masses^{5,17}, (4) A plant-nutrient model³⁰ is assigned to the basal trophic level⁵. These steps were repeated independently 600 times to generate realistic variation in model parameters defining network structure, predator metabolism, maximum consumption, initial biomass, and functional response, and the nutrient uptake rates of basal species (Full Methods). To analyze the effect of removing each species on the biomass of every other species, each of the 600 dynamic network models was run once with all species present and subsequently with each species in the network removed in turn. Each species average biomass per unit area and population density (number of individuals per unit area) from time step 50 to 200 was monitored to calculate I and *per capita I* (see Supplement). For each removal, we tracked 90 attributes of the global network (e.g., connectance), the local network structure (e.g., the numbers of direct consumers), the species (e.g., body mass and biomass of T and R), and the pair (e.g., degrees separated) (see Full Methods). CART was used to model the sign and magnitude of I and to select explanatory variables for Reduced Major Axis (RMA) regression and multiple linear regression models of $\log|I|$ and $\log|per\ capita\ I|$. Empirical data on interaction strengths in a rocky

intertidal community were re-analyzed from previously published data^{22,28} (see Full Methods).

Full Methods and any associated references are available in the online version of the paper at www.nature.com/nature.

Full Methods

Dynamic Model. Our model of population dynamics is consistent with prior analyses of “keystone” species removal in complex networks⁸, with three modifications: 1) We use a generalized version of the functional response, F_{ij} , describing the realized fraction of species i 's maximum rate of consumption spent consuming species j :

$$F_{ij} = \frac{\omega_{ij} B_j^h}{B_0^h + c B_i B_0^h + \sum_{k=\text{resources}} \omega_{ik} B_k^h}, \quad (2)$$

where ω_{ij} is the fraction of i 's maximum consumption rate targeted to consuming j , B_0 is the half saturation density of i , h is the Hill-exponent which regulates the shape of the curve from Holling Type II to Holling Type III³¹. The parameter c quantifies consumer (predator) interference: if $c > 0$ ^{references32-34} individuals in population i interfere with each other, reducing *per capita* consumption. In contrast to prior work⁵ based on Type II F_{ij} , we varied h and c randomly, independently according to normal distributions (mean = 1.5, SD = 0.25 for h ; mean = 0.5, SD = 0.25 for c). We used uniform relative consumption rates for consumers with n resources ($\omega_{ij} = 1/n$, $B_0 = 0.5$) – that is, consumers feed on resources in proportion to the relative biomasses of those resources. 2) We did not constrain the number of basal (autotroph) species to five as in prior work⁵, and we created a random competitive hierarchy amongst basal species by randomly varying the half-saturation densities determining their nutrient uptake uniformly between 0.1 and 0.2. 3) Consumer's metabolic and maximum consumption varied randomly because consumer-resource body mass ratios and the consumer-resource interaction structure that defines a species trophic level were random. All other model parameters are consistent with prior work^{5,17}.

Simulations. Each simulation started with random initial biomass densities B_i selected independently, uniformly from the interval (0.05, 1). Each network was simulated once with all initial species present (Control), and once with each species removed

independently, a total of (species present)+1 times. In each simulation, the biomass of each species was averaged from time step 50 to 200 (see Supplementary Information) to yield a “removal matrix” for all species showing how each species’ time-averaged biomass differs with and without each of the other species. Many measures of this change have been used^{35,36}. Here we use the difference in T biomass with and without R because it is transparent and can be used to derive other measures.

Species with biomass density less than 10^{-30} after 200 time steps were considered extinct. Species that went extinct in the control runs were excluded from analysis. All 600 networks were persistent over 200 time steps: 16 networks lost one species, and 1 network lost 2 species in the control runs, yielding measurements of over 254,032 species interactions among 12,116 species (See Supplementary Information for results of structural extinctions and longer time series).

Simulation Data Analysis. We tracked four broad categories of explanatory variables.

1) Global web structure³⁷: initial and final species richness; initial and final connectance; number and proportion of top (t), intermediate (i), and basal (b) species; number and proportion of herbivores, carnivores, and omnivores; number of links between $t-i$, $t-b$, $i-b$ and $i-i$, the total number of links and number of links per species; the mean, maximum, and standard deviation of the web’s resource-averaged trophic level³⁸, the mean, maximum, and standard deviation of shortest chain between each species and a basal species; and the clustering coefficient of the web³⁹. **2) Local network structure around R and T :** resource-averaged trophic level and the number, total biomass, mean vulnerability (i.e., number of consumer species), and mean generality (i.e., number of resource species) of both consumer and resource species that are one, two, and three degrees from the R and T of each interaction. **3) R and T attributes:** mean biomass before R removal, mean body mass, consumer functional response shape (Hill coefficient), consumer interference, and the relative half saturation

concentration of nutrient uptake for producers. **4) Attributes of the R - T pair:** degrees of separation, “simple” vs. “diffuse” connections (i.e., single vs. multiple paths from R to T), the net sign of all shortest paths (SP) and next-shortest paths (NSP) between R and T , the sum $SP + NSP$, and the weighted sum $SP + NSP/2$. The sign of each path of a given length was determined by multiplying the signs of each link along the path, where all consumer-to-resource links are negative and resource-to-consumer links are positive. For diffuse connections, the signs of multiple paths of the same length were summed (+1 for positive and -1 for negative effects)⁴⁰. These variables were used to predict the sign and magnitude of the interaction between R and T . Both positive and negative I and *per capita I*, as well as the biomass, body mass, and density of R and T were all approximately log-normally distributed (e.g., Supplementary Fig. S3).

To model I , we applied CART⁴¹, a nonlinear modelling algorithm, to data from a random sample of half the webs (training data). Because the distribution of $|I|$ is roughly lognormal (Fig. S3), the quadratic prediction error that CART seeks to minimize (by recursively “splitting” the data) is dominated by the tails of the distribution of I . Therefore, we allowed CART to split the data until a terminal leaf captured points with a mean I within the 95th percentile of $|I|$. In the resulting tree ($R^2 = 0.86$) $|I|$ and the sign of I were predicted by different sets of variables, and these results were used to guide subsequent analyses on log-transformed $|I|$. The models were then tested on the other 300 webs (test data). When modelling *per capita I*, we had an *a priori* interest in understanding how body size, which drives *per capita* maximum consumption rates for all species, explains variation in *per capita I* in a realistically complex community. We first used Reduced Major Axis regression to quantify the relationship between $\log|per\ capita\ I|$ and $\log(R_{body_mass})$. To examine the influence of the network on this relationship, we first examined simply connected one degree effects of specialist consumers on resources that have only one consumer. We then included all diffuse one degree effects of consumers on their resources, and finally all possible interactions in

the community. We then used CART to explore which of the remaining variables explain the residuals of the $\log_{10}|per\ capita\ I|$ vs. $\log_{10}(R_{body_mass})$ regression. These additional variables were combined with $\log(R_{body_mass})$ in a multiple linear regression to predict $\log|per\ capita\ I|$. As before, the models were built using half the webs, selected at random, and tested on the other half.

Experimental Data. The data re-analyzed here measure the effects of predatory whelks, *Nucella emarginata*, on one of their primary resources, the mussel *Mytilus edulis*, both in the presence and absence of an alternative resource, the acorn barnacle *Balanus glandula* on the rocky, central coast of Oregon, USA, in mid-intertidal disturbance patches^{22,28}. We quantified *per capita* and population *I* between whelks (*R*) and mussels (*T*) with barnacles present and absent, for each of two whelk biomass enclosure levels (high and low). To compare experimental results with our simulations, separate interaction strengths were estimated for each year of each of the three experiments by using the time-averaged mussel biomass in each replicate of each treatment. Replicates and experimental runs were spatially and/or temporally independent, and there was no consistent correlation in the time-averaged *I* across years (*r* ranged from 0.13 to -0.78). Thus, the experiment provided repeated estimates of interaction strength across natural variation in mussel and barnacle recruitment with space and time. Since all plots were initially scraped, data from the transient colonization phase were excluded from the analysis. Mussel biomass data used to predict *I* were from plots that enclosed whelks, which we considered analogous to the ‘*R* present’ condition of our simulation data. To compare the empirical results with our simulations, we converted the empirical data to relative biomass density and used the

linear regression model that predicts *per capita I* in the ATN simulations: $\log_{10}[\textit{per capita I}] = -1.14 + (0.88 * \log_{10}(R_{\text{body_mass}})) + (0.71 * \log_{10}(T_{\text{biomass}})) - (0.79 * \log_{10}(R_{\text{biomass}}))$ (Fig. 2c). One percent cover of mussels in the 400 cm² plots was the minimum biomass density unit. Mussels generally formed a mono-layer, so we assumed their biomass increased linear with cover. We used photos of the experimental plots to estimate that one percent mussel cover for this plot size was approximately 2-4 young mussels and that the body size ratio of whelks to mussels was approximately two. In the treatments that included non-trophic interactions mediated through barnacles, the difference between the model predictions and the data were regressed against total barnacle cover in the paired ‘barnacle recruitment’ plots.

References

- 1 Yodzis, P., *Ecology* **69**, 508-515 (1988).
- 2 Carbone, C., Teacher, A. & Rowcliffe, J., *PLOS Biology* **5**, e22 (2007).
- 3 Yodzis, P. & Innes, S., *Am. Nat.* **139**, 1151-1175 (1992).
- 4 Alon, U., *Nature* **446**, 497-497 (2007).
- 5 Brose, U., Berlow, E. L. & Martinez, N. D., *Ecology Letters* **8**, 1317-1325 (2005).
- 6 Dunne, J. A., Williams, R. J. & Martinez, N. D., *Ecology Letters* **5**, 558-567 (2002).
- 7 Ebenman, B., Law, R. & Borrvall, C., *Ecology* **85**, 2591-2600 (2004).
- 8 Sole, R. & Montoya, J., *Proceedings of the Royal Society of London Series B-Biological Sciences* **1480**, 2039-2045 (2001).
- 9 Bascompte, J., Melian, C. J. & Sala, E., *Proceedings of the National Academy of Sciences of the United States of America* **102**, 5443-5447 (2005).
- 10 Ives, A. R. & Cardinale, B. J., *Nature* **429**, 174-177 (2004).
- 11 Brown, J. H., Gillooly, J. F., Allen, A. P., Savage, V. M. & West, G. B., *Ecology* **85**, 1771-1789 (2004).
- 12 Woodward, G. et al., *Trends in Ecology & Evolution* **20**, 402-409 (2005).
- 13 Reuman, D. C. & Cohen, J. E., in *Advances in Ecological Research, Vol 36* (2005), Vol. 36, pp. 137-182.
- 14 Menge, B. A., *Ecol. Monogr.* **65**, 21-74 (1995).
- 15 Peacor, S. D. & Werner, E. E., *Ecology* **78**, 1146-1156 (1997).
- 16 Harte, J., *Ecology* **85**, 1792-1794 (2004).
- 17 Brose, U., Williams, R. J. & Martinez, N. D., *Ecology Letters* **9**, 1228-1236 (2006).
- 18 Otto, S. B., Rall, B. C. & Brose, U., *Nature* **450**, 1226-1229 (2008).
- 19 Brose, U. et al., *Ecology* **87**, 2411-2417 (2006).
- 20 Williams, R. J. & Martinez, N. D., *Nature* **404**, 180-183 (2000).
- 21 Srivastava, D. S. & Vellend, M., *Annual Review of Ecology Evolution and Systematics* **36**, 267-294 (2005).
- 22 Berlow, E. L., *Nature* **398**, 330-334 (1999).
- 23 Power, M. E. & Mills, L. S., *TREE* **10**, 182-184 (1995).
- 24 Wootton, J. T. & Emmerson, M., *Annual Review of Ecology Evolution and Systematics* **36**, 419-444 (2005).
- 25 Strong, D. R., *Ecology* **73**, 747-754 (1992).
- 26 McCann, K., Hastings, A. & Huxel, G. R., *Nature* **395**, 794-798 (1998).
- 27 Neutel, A.-M., Heesterbeek, J. A. P. & De Ruiter, P. C., *Science* **296**, 1120-1123 (2002).
- 28 Berlow, E. L., *Ecol. Monogr.* **67**, 435-460 (1997).
- 29 Pascual, M., *Plos Computational Biology* **1**, 101-105 (2005).
- 30 Huisman, J. & Weissing, F. J., *Nature* **402**, 407-410 (1999).
- 31 Real, L., *Am. Nat.* **111**, 289-300 (1977).
- 32 Beddington, J. R., *Journal of Animal Ecology* **44**, 331-340 (1975).
- 33 DeAngelis, D. L., Goldstein, R. A. & O'Neill, R. V., *Ecology* **56**, 881-892 (1975).
- 34 Skalski, G. T. & Gilliam, J. F., *Ecology* **82**, 3083-3092 (2001).

- 35 Navarrete, S. A. & Menge, B. A., *Ecol. Monogr.* **66**, 409-429 (1996).
36 Berlow, E. L. et al., *J Anim Ecology* **73**, 585-598 (2004).
37 Dunne, J. A., Williams, R. J. & Martinez, N. D., *Marine Ecology-Progress
Series* **273**, 291-302 (2004).
38 Williams, R. J. & Martinez, N. D., *Am. Nat.* **163**, E458-E468 (2004).
39 Williams, R. J., Martinez, N. D., Berlow, E. L., Dunne, J. A. & Barabási, A.-L.,
Proceedings of the National Academy of Science **99**, 12913-12916 (2002).
40 Jordan, F., Liu, W. C. & Davis, A. J., *Oikos* **112**, 535-546 (2006).
41 De'ath, G. & Fabricius, K. E., *Ecology* **81**, 3178-3192 (2000).

Supplementary Information accompanies the paper at www.nature.com/nature.

Acknowledgements This project was funded by grants from the German Research Foundation (BR 2315/1-1,2,3) to U.B. and an Alexander Humboldt Foundation Fellowship to E.L.B. This study benefited enormously from invaluable discussions with S. Scheu, O. Petchey, J. L. Green, and L M. Kueppers, the PEaCE Lab, and the EcoNetLab. We are grateful to B. A. Menge, S. D. Hacker, S. A. Navarrete, and E. A. Wieters for providing data on mussel and whelk body mass and biomass.

Author Contributions The first (E.L.B) and last (U.B.) authors equally contributed the most to this work.

Author Information Correspondence and requests for materials should be addressed to E.L.B. (e-mail: eberlow@ucmerced.edu). The authors declare no competing financial interest.

Fig. 1 | Explaining variation in the magnitude and sign of I . Untransformed population-level I as a function of **a**, the degrees of separation between R and T , and **b**, $\log_{10}(T_{\text{biomass}})$. Coloured symbols highlight all the CART leaves whose mean was within the top 5% strongest I . Strong negative I included one degree, “simple” (one path) effects of R on basal T where R is T 's only consumer (dark red) or one of two consumers (orange), or “diffuse” (multiple paths) effects of high biomass R on high biomass T where the weighted sum of path signs < 0 (yellow). Strong positive I included simple effects of high biomass R on high biomass T (purple), and diffuse effects of high biomass R on high biomass T where the weighted sum of path signs ≥ 0 (blue and green). **c and d**, The same data as **b**, but with $\log_{10}|I|$ on the y-axis. Colour codes in **c** are the same as in **a** and **b**. Colours in **d** indicate upper (light red) and lower (blue) 50% quantiles of R_{biomass} . Multiple linear regression: $\log_{10}|I| = -1.34 + 0.71 \log_{10}(T_{\text{biomass}}) + 0.22 \log_{10}(R_{\text{biomass}})$, $R^2=0.65$ and 0.63 in the training and test data, respectively.

Fig. 2 | Body mass scaling and *per capita* interaction strengths. **a**, Maximum *per capita* consumption as a function of body mass (input parameters); colours indicate increasing consumer generality from yellow to red; RMA regression: slope = 0.74 ± 0.003 (mean \pm 95% CI), $R^2 = 0.90$, $n = 37,600$ direct consumer-resource interactions. **b**, $\log_{10}|per\ capita\ I|$ depending on $\log_{10} R_{\text{body_mass}}$. Contour lines indicate 10% density quantiles from blue (low) to red (high). RMA regression model: slope = 1.38 , $R^2 = 0.46$. **d**, Observed $\log_{10}|per\ capita\ I|$ versus that predicted from the multiple linear regression: $\log_{10}|per\ capita\ I| = -1.14 + 0.88 \log_{10}(R_{\text{body_mass}}) + 0.71 \log_{10}(T_{\text{biomass}}) - 0.79 \log_{10}(R_{\text{biomass}})$, $R^2 = 0.88$. Colours are the same as in Fig. 1d.

Fig. 3 | More complex is more simple. The proportion of variation in (a) $\log_{10}|I|$ and (b) $\log_{10}|per\ capita\ I|$ explained by the most parsimonious multiple linear regressions described in Figs. 1d and 2c for different levels of species richness that each included a range of connectance values. The absolute magnitude of both I and $per\ capita\ I$ explained increases with web size ($R^2 = 0.74$ and 0.88 for a and b respectively). Note that increasing connectance alone for a given level of diversity had no clear effect on the variation explained.

Fig. 4 | Empirically testing the metabolic baseline of interaction strengths.

$\log_{10}|per\ capita\ I|$ of predatory whelks (R) on mussels (T) depending on $\log_{10}(T_{biomass})$ for low (blue) and high (red) levels of $R_{biomass}$ with (a) or without (b) non-trophic influences of barnacles. ATN model predictions (dotted lines) are compared to separate linear regressions through the empirical data (solid lines). In the interaction web diagrams, solid arrows indicate trophic interactions, and dotted arrows indicate non-trophic interactions. Regression models for the empirical data (solid lines) for a: $R^2 = 0.48$, $p < 0.0001$, $\log_{10}(|per\ capita\ I|) = -0.29 + 0.77 \log_{10}(T_{biomass}) - 0.47 \log_{10}(R_{biomass})$; b: $R^2 = 0.22$, $p = 0.03$, $\log_{10}|per\ capita\ I| = 0.47 + 0.13 \log_{10}(T_{biomass}) - 0.96 \log_{10}(R_{biomass})$. c, The difference between empirically observed $\log|per\ capita\ I|$ when non-trophic influences of barnacles are present and those predicted by the ATN simulations as a function of mean barnacle cover in paired plots without whelks or mussels. RMA regression: slope = -0.025 , $R^2 = 0.26$, $p = 0.002$.

Figure 1

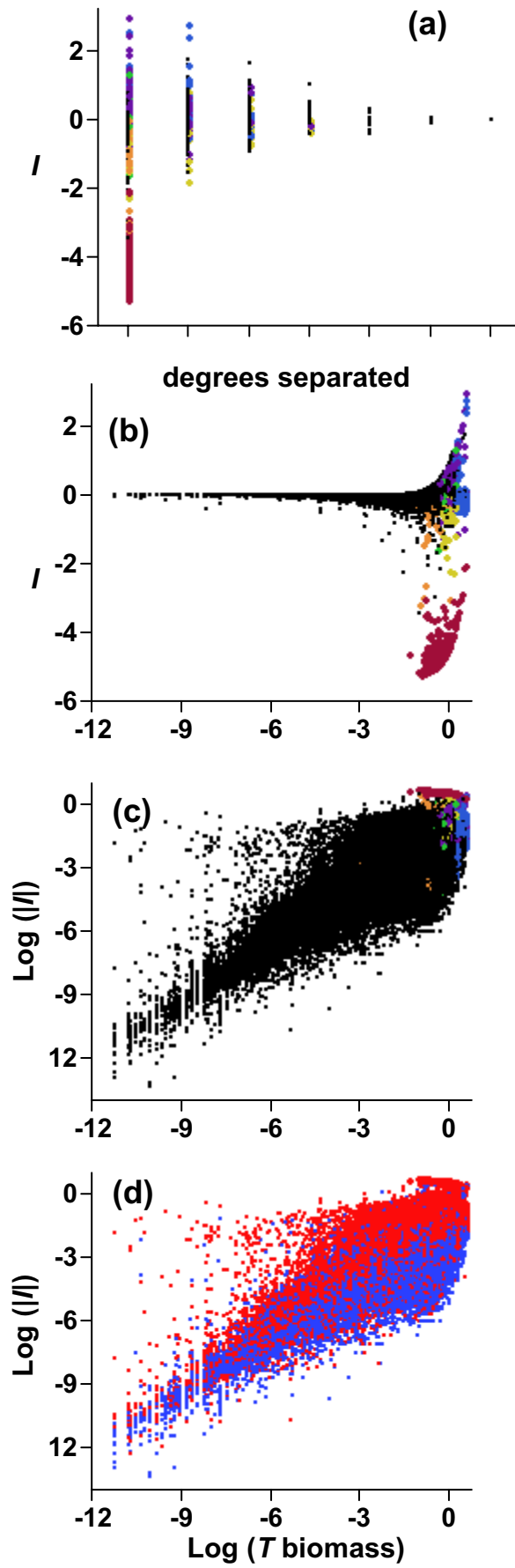


Figure 2

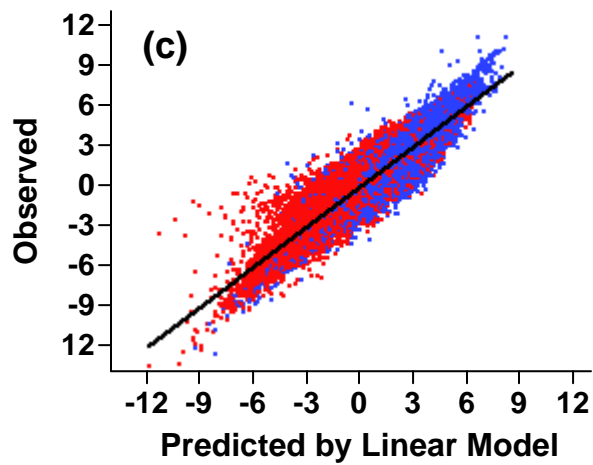
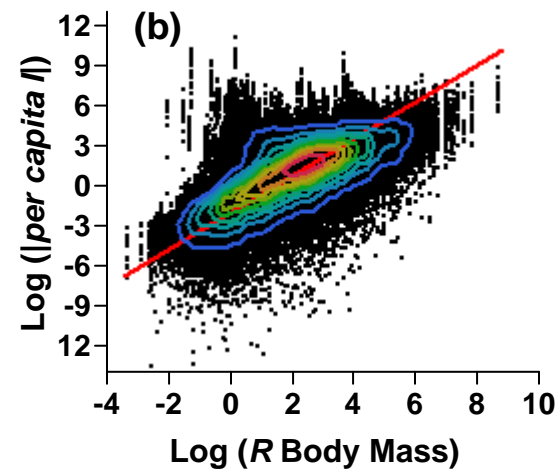
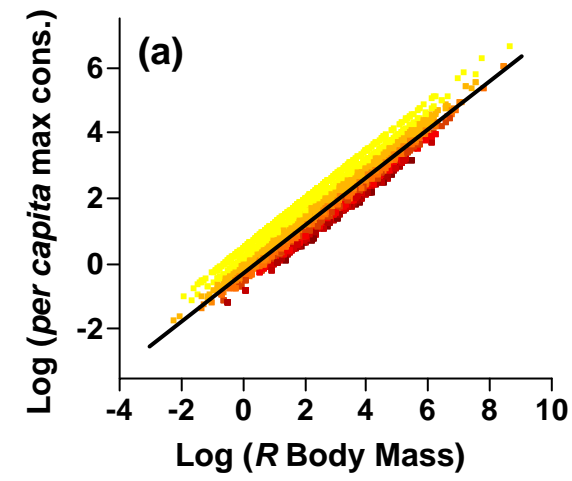


Figure 3

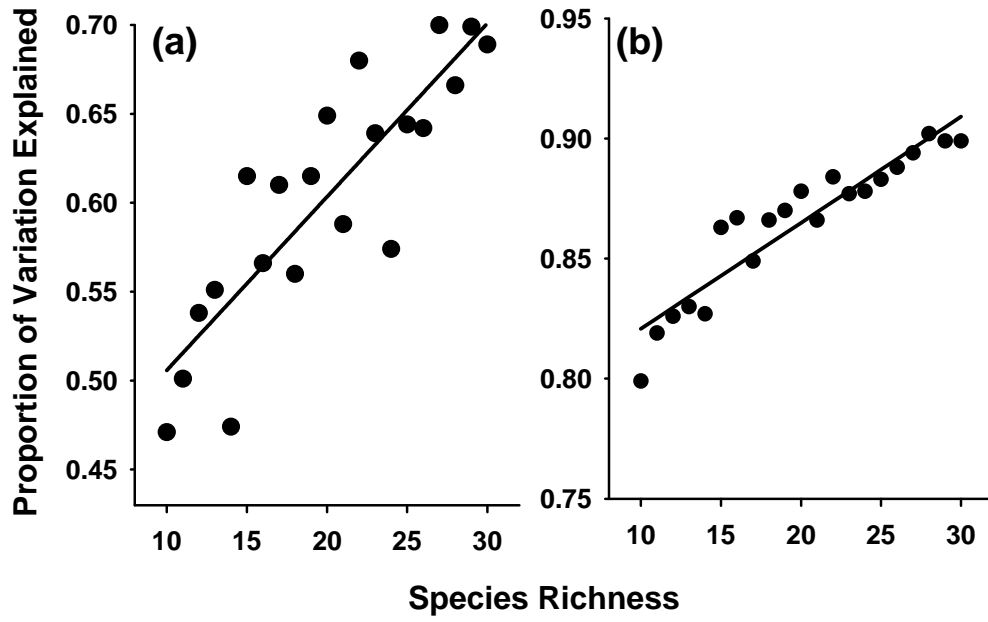


Figure 4

